Degradation of textile dyes Remazol Yellow Gold and reactive Turquoise: optimization, toxicity and modeling by artificial neural networks

Graziele Elisandra do Nascimento, Daniella Carla Napoleão, Rayany Magali da Rocha Santana, Lívia Vieira Carlini Charamba, Julierme Gomes Correia de Oliveira, Maiara Celine de Moura, Luana Cassandra Breitenbach Barroso Coelho and Marta Maria Menezes Bezerra Duarte

ABSTRACT

In this work, the degradation of Remazol Yellow Gold RNL-150% and Reactive Turquoise Q-G125 were investigated using AOP: photolysis, UV/H_2O_2, Fenton and photo-Fenton. It was found that the photo-Fenton process employing sunlight radiation was the most efficient, obtaining percentages of degradation above 87%. The ideal conditions for the degradation of the dyes were determined from a factorial design 2^3 and study of the [H_2O_2] ([H_2O_2] equal to 100 mg·L^{-1}); [Fe] equal to 1 mg·L^{-1} and pH between 3 and 4. In the kinetic study, a degradation of more than 97% was obtained after 150 min for the chromophoric groups and 91% for the aromatic compounds. The experimental data obtained presented a good fit to the nonlinear kinetic model. The model of artificial neural networks multilayer perceptron (MLP) (4-11-5) using the software Statistica 8.0 enabled the modeling of the degradation process and showed a better prediction of the data. The toxicity to the seeds of *Lactuca sativa* and the bacteria *Escherichia coli* and *Salmonella enteritidis* allowed to evaluate the effectiveness of the process. The results of this study suggest that the use of photo-Fenton process with sunlight radiation is an effective way to degrade the dyes under study.

Key words | advanced oxidative processes, artificial neural networks, kinetic, textile dyes, toxicity

Graziele Elisandra do Nascimento
(corresponding author)
Daniella Carla Napoleão
Rayany Magali da Rocha Santana
Lívia Vieira Carlini Charamba
Marta Maria Menezes Bezerra Duarte
Departamento de Engenharia Química,
Universidade Federal de Pernambuco,
Recife,
Brasil
E-mail: *grazielen@yahoo.com.br*

Julierme Gomes Correia de Oliveira
Departamento de Engenharia Química,
Faculdade Boa Viagem,
Recife,
Brasil

Maiara Celine de Moura
Luana Cassandra Breitenbach Barroso Coelho
Departamento de Bioquímica,
Universidade Federal de Pernambuco,
Recife,
Brasil

INTRODUCTION

Effluents from textile industries are a source of environmental concern in terms of toxicity and persistence of their substances (Le *et al.* 2016). These effluents contain a variety of organic pollutants, including dyes, which are generated from different operations of the textile process, such as washing, bleaching and dyeing (Ozturk *et al.* 2009).

Synthetic dyes have a variety of chemical structures and compositions that can be toxic (Divya *et al.* 2013). These compounds have been highlighted as dangerous substances, since they are stable to light and heat, being considered recalcitrant and resistant to biodegradation (Ertugay & Acar 2017). The presence of dyes in the receptor bodies affects the absorption and reflection of sunlight through water, reducing the solubility of oxygen and threatening the photosynthetic activity of aquatic plants and algae (Mane & Vijay Babu 2011). Moreover, synthetic dyes emitted with industrial effluents have a bioaccumulative effect, causing short term damage to the environment (Barros *et al.* 2014). Thus, these effluents must be treated before they are released into the environment.

Many research methods for the removal of synthetic dyes, including the physical and biological have been proposed. In the physical methods, the pollutants are transferred from one phase to another without any degradation, and there is a need to treat the solid residue generated (Shu *et al.* 2013). Biological methods have not been shown to be effective in the degradation of these compounds due to their resistant and stable biodegradation structures (Annadurai *et al.* 2003). Therefore, the use of a

doi: 10.2166/wst.2018.251

more efficient process is necessary for the degradation of these pollutants.

In this context, advanced oxidative processes (AOP) have been emerging as effective and consolidated technologies for the treatment of effluents for the removal of non-treatable organic pollutants by means of conventional techniques (Fahimirad *et al.* 2017).

Lima *et al.* (2016) evaluated the application of the process (UV/H_2O_2) in the degradation of commercial blue Azo dye 5G using UV-H_2O_2 with a discoloration of 91.8% after 30 min of treatment. Sreeja & Sosamony (2016) used the photo-Fenton process to investigate the treatment of synthetic textile wastewater, achieving 82% of color removal. Ertugay & Acar (2017) investigated the degradation of Direct Blue 71 by Fenton process and obtained 94% dye removal after 20 min of reaction.

In order to evaluate the efficiency of these treatments, it is also important to perform toxicity tests, since the toxicity of the textile effluents is associated with the dyes and their degradation products (Punzi *et al.* 2015). It is also essential to verify the adjustment of experimental data to mathematical modeling using both kinetic models and empirical models, such as artificial neural networks (ANNs).

Eskandarloo *et al.* (2016) predicted the degradation efficiency of Fuchsin Acid (AF) and Malachite Green (MG) dyes using ANN for the hybrid process UV/Fe^{2+}/H_2O_2/TiO_2-SiO_2. Speck *et al.* (2016) compared the predictive capacity of the response surface methodology (RSM) and ANN in the modeling of photo-Fenton degradation of Rhodamine B dye (Rh-B). Thus, more detailed studies on AOP are needed since many variables and responses are involved in these processes.

The present work was developed with the purpose of evaluating the AOP in the degradation of the azo textile dyes Remazol Yellow Gold 150% and Turquoise Reactive QG 125. For this, studies were carried out on the variables involved in the process, as well as the suitability of existing kinetics models and proposition of a mathematical modeling using ANN.

METHODOLOGY

Dyes

Remazol yellow gold RNL-150% (RYG) (CI name: Reactive Orange 107; CAS number: 90597-79-8/12220-08-5) and Turquoise reactive Q-G125 (TR) (CI name: Reactive Blue 21; CAS number: 12236-86-1/73049-92-0) dyes were supplied by DyStar and Texpal companies, respectively. The working matrix was prepared from an aqueous solution containing the textile dyes under study at the concentration of 50 mg·L^{-1} of each dye.

Reagents

All reagents used throughout this study were analytical grade and without further purification. Ferrous sulfate heptahydrate ($FeSO_4.7H_2O$, 99.9% purity, Vetec) was used as the source of iron and hydrogen peroxide (H_2O_2, 30% v/v, Química Moderna) as an oxidizing agent. The pH of the solutions were adjusted using H_2SO_4 1 mol·L^{-1} (97% purity, Merck). All solutions were prepared with deionized water.

Analytical method

A UV/visible spectrophotometer (Thermoscientific, Genesys 10S) operating in wavelength range between 190 and 1,100 nm was used to determine the characteristic wavelengths (λ) of each dye studied. The quantification of the compounds before and after the degradation process was performed based on the construction of analytical curves (for each selected λ), with a linear concentration range of 2 to 100 mg·L^{-1}, from stock solutions of each dye at the concentration of 100 mg·L^{-1}. Then, the limits of detection (*LOD*) and quantification (*LOQ*) and coefficient of variation (*CV*) were determined according to Cgcre (2016).

Evaluation of degradation by different processes

In order to identify the type of AOP that has the highest degradation efficiency of the dyes under study, the following processes were tested: photolysis, UV/H_2O_2, Fenton and photo-Fenton. The degradation tests were carried out on benchtop photochemical reactors, the first one using light bulb (OSRAM) with a power of 300 W (Santana *et al.* 2017) and the second equipped with three UV-C lamps, arranged in parallel, with a power of 30 W (Zaidan *et al.* 2017), and also the solar radiation. For each case, the emission of photons was measured using a radiometer (Empórionet).

The tests to evaluate the different processes were carried out under the following conditions: iron concentration ([Fe] = 5 mg·L^{-1}); concentration of hydrogen peroxide ([H_2O_2] = 50 mg·L^{-1}), pH between 5 and 6 (natural solution) and an exposure time of 1 h. For the experiments, beakers with 100 mL capacity were used, to which 50 mL of the mixture containing the two dyes were added.

Factorial design

Selecting the most efficient AOP in the degradation of the dyes from the previous study, a factorial design 2^3 was carried out with central point, to evaluate the influences of the variables [H_2O_2] (100, 150 and 200 mg·L^{-1}), [Fe] (1, 3 and 5 mg·L^{-1}) and pH (3–4, 4–5 and 5–6) on the process and to define the working conditions. The tests were performed in random order and the central point in triplicate, totaling 11 experiments.

The response used to determine the efficiency of the process was the percentage of degradation of the dyes. The calculations of the effects of the factors and the interactions between them with their respective standard errors were made according to Barros Neto *et al.* (2007), using Statistica for Windows 8.0 software.

Optimization of the hydrogen peroxide concentration

With the results of the factorial design, the optimization step of the variable [H_2O_2] was carried out. This step had the objective of reducing costs, based on the necessary use of the reagent without excess. The evaluation was carried out in the time of 1 h at the best level of [Fe] and pH found in the factorial design and by varying the [H_2O_2]: 50, 80, 100, 120, 140, 150, 180 and 200 mg·L^{-1}.

Kinetic study and modeling

Optimized the working conditions, the kinetic study of the degradation of the dyes was carried out in the following times: 25; 35; 45; 55; 65; 75; 85; 100; 120 and 150 min. The assays were performed at a temperature of 25 ± 1 °C, at a pressure of 1 atm, for 1 L of the dye solution, and 10 mL aliquots removed.

Then, the adjustment of the experimental data obtained to the kinetic model proposed by Chan & Chu (2003), presented in Equation (1), was verified.

$$C = C_0\left(1 - \frac{t}{\rho - \sigma t}\right) \quad (1)$$

in which C is the concentration of the dye (mg·L^{-1}) after a time of t (min) and C_0 is the initial concentration of the dye (mg·L^{-1}). The parameters ρ and σ represent the reaction kinetics (min) and the oxidative capacity of the system (dimensionless), respectively.

An estimation of the dye conversion (discoloration efficiency) was also performed based on Equation (2).

$$X = 100\left(1 - \frac{C_f}{C_0}\right) \quad (2)$$

in which X is the conversion (%), C_0 and C_f are the initial and final concentrations of the solution (mg·L^{-1}), respectively.

Artificial neural network modeling

The neural network was implemented through Statistica 8.0 software in order to model the data obtained experimentally. Two different networks were tested: multilayer perceptron (MLP) and radial basis function (RBF). The activation functions employed were identity, logistics, hyperbolic and exponential, with a limited amount of neurons in the hidden layer between 3 and 15 and with a maximum of 1,000 interactions. Sampling was performed randomly by the software with percentages of train, test and validation of 70%, 15% and 15%, respectively. The input data for the neural network were: time (min), pH, [H_2O_2] (mg·L^{-1}) and [Fe] (mg·L^{-1}); and the output data were: percentage of degradation at the λ of 239, 339, 411, 625 and 661 nm. At the end, Statistica 8.0 retained only the 10 best ANNs and the two best ones were chosen according to the linear regression coefficient (R^2).

Seeds toxicity

The toxicity tests were performed under the same conditions of the kinetic study, after submission of the dye solution to the radiation for 100 min. The toxicity evaluation consisted in the exposure of lettuce seeds (*Lactuca sativa*) to different concentrations of the solution containing the dyes. Concentrations of the solution were used without treatment and after treatment, the latter in the following percentages: 100, 70, 50, 10, 5 and 1%. Ten seeds were added together with 2 mL aliquots of each solution. All analyses were performed in triplicate.

In the sensitivity tests, the negative and positive controls were, respectively, water and 3% boric acid solution, in volumes equal to that of the mixture. The temperature range used in the toxicity tests was 25 ± 1 °C, with the Petri dishes being kept in an environment with no light for a period of 120 h. After that period, the number of seeds that germinated in the positive and negative controls was

evaluated, and compared to the germinated quantity in the concentration of each plate. Afterwards, root growth was observed, whose radical size was measured with the aid of a pachymeter.

Thus, the relative growth index (*RGR*) and the germination index (*GI*) were calculated, as shown in Equations (3) and (4), respectively (Young *et al.* 2012).

$$RGR = \frac{RLS}{(RLC)} \tag{3}$$

$$GI = \frac{RGR(SGS)}{(SGC)} \tag{4}$$

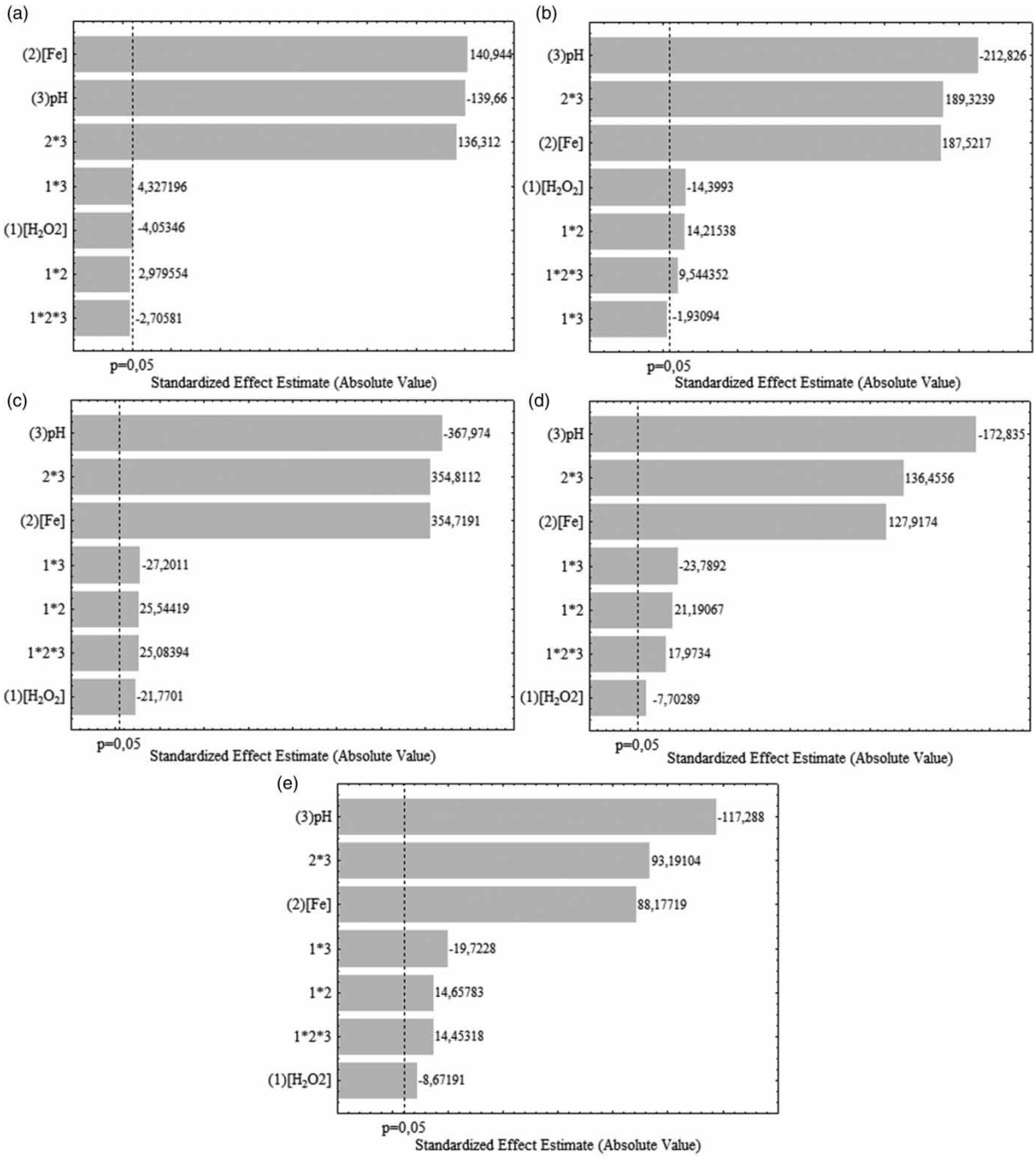

Figure 1 | Pareto charts for the λ: (a) 239 nm, (b) 339 nm, (c) 411 nm, (d) 625 nm and (e) 661 nm.

in which *RLS* is the total root length in the sample; *RLC*, the total root length in the negative control; *SGS*, the number of seeds germinated in the sample; and *SGC* the number of seeds germinated in the negative control.

For a better evaluation of the toxicity of the compounds under study, another study was carried out against two bacteria using the same conditions of the test with the seed.

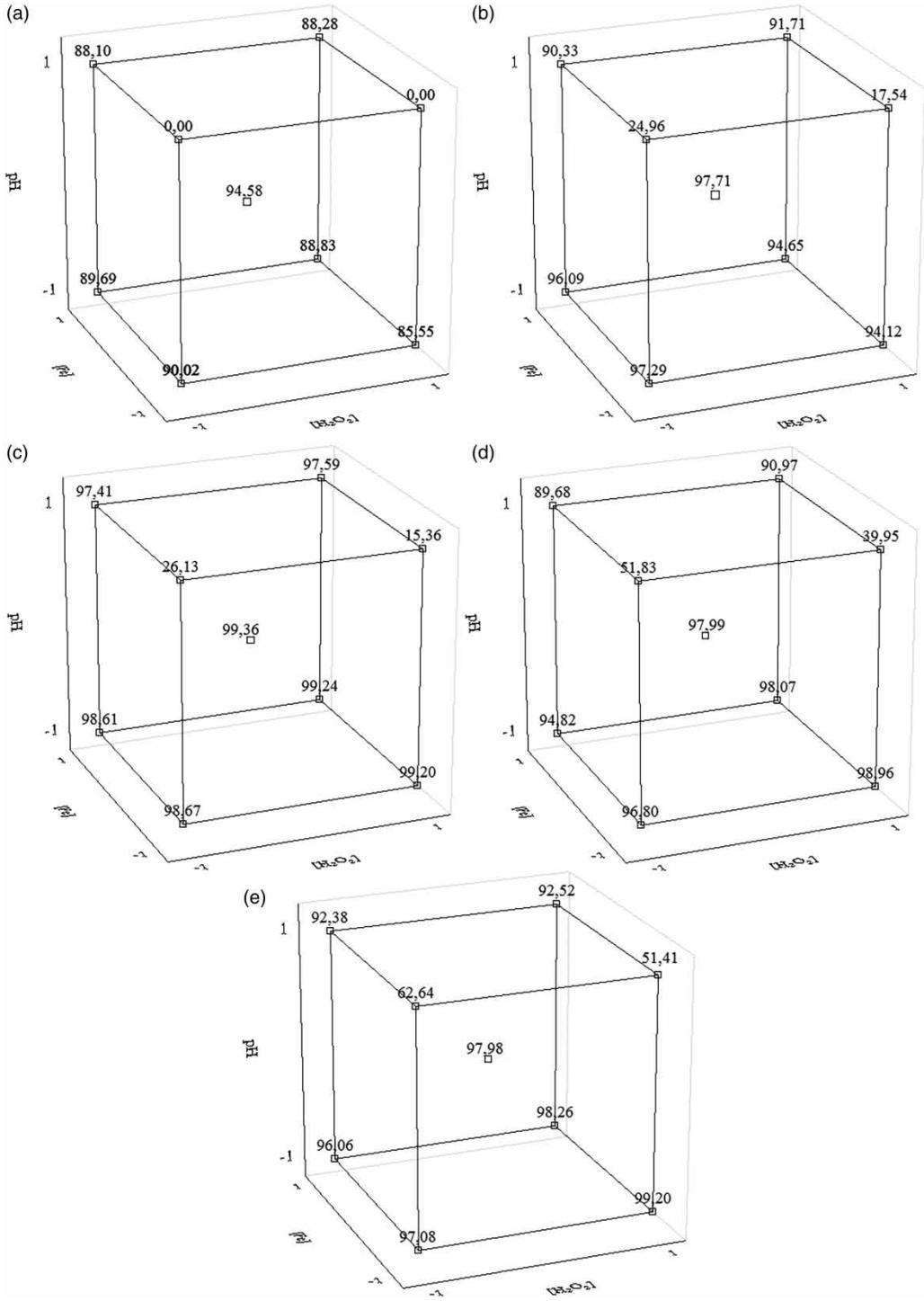

Figure 2 | Cube graphs for the λ: (a) 239 nm, (b) 339 nm, (c) 411 nm, (d) 625 nm and (e) 661 nm.

Bacteriological toxicity

The microbiological toxicity test was performed with the untreated and post-treatment dye solutions (1%, 5%, 10%, 50%, 70% and 100%) before and after the dilution of 1:10 (10^{-1}) in sterile ultrapure water. Each sample (450 μL) was incubated for 24 h at 36 °C with the suspension of *Escherichia coli* UFPEDA 224 and *Salmonella enteritidis* UFPEDA 414/MM 6247 (50 μL; 10^5 UFC·mL^{-1}em NaCl 0,15 mol·L^{-1}) and Mueller Hinton broth medium (100 μL). The negative control corresponded to bacterial cells treated with sterile ultrapure water. Before and after the incubation period, the contents of each treatment were transferred to 96-well microtiter plates for reading at 600 nm (DO_{600}) to determine the growth percentage that was compared to the negative control. In addition, aliquots of the treatments were seeded in Petri dishes containing Mueller Hinton Agar (MHA) medium for evaluation of cell viability after 48 h of incubation at 36 °C. Each assay was performed in triplicate and three independent experiments were performed.

RESULTS AND DISCUSSION

Dyes identification

Samples were read in a UV-Vis spectrophotometer and allowed to verify the λ of maximum absorbance of RYG and TR dyes. Five λ of maximum absorbance were found: 239, 339, 411, 625 and 661 nm. The first one refers to the aromatic groups and the others to the chromophoric groups. From the construction of the analytical curves for each identified wavelength were obtained: $LOD < 0.13$ mg·L^{-1}, $LOQ < 0.49$, as well as *CV* less than 2.42 and *r* equal of 0.99.

According to CGCRE (2003), correlation coefficients (*r*) higher than 0.90, indicates a good linearity of the method. As well, the values of coefficients of variation that were smaller than 2.5% show a good precision of the methodology used. According to Harris (2001), the lower the value of the CV, the more precise will be the series of measures.

Evaluation of the degradation employing different AOP

The efficiency of the process was measured in terms of the percent degradation of the aqueous solution containing the dyes. The photon emissions of each reactor were equal to a 4.00×10^6 W·m^{-2} for sunlight, 1.44×10^{-3} W·m^{-2} for UV-C and a variation of 2.06×10^4 to 12.16×10^4 W·m^{-2} for radiation solar.

The photolysis and UV/H_2O_2 processes failed to promote the degradation of the studied dyes (less than 5%). It was found that the Fenton and photo-Fenton processes using UV-C radiation were not efficient in the degradation of the dyes. The percentages of degradation values for these processes were between 3.54 and 70.52% and 68.13 and 93.57%, respectively. Comparing the photo-Fenton process using solar radiation and sunlight, there was a percentage difference of 3.86% and 5.32% in relation to λ 625 and 661 nm, respectively. However, for the λ of 239, 339 and 411 nm, this percentage difference was less than 1.3%. Thus, the photo-Fenton process using sunlight radiation was selected for subsequent studies, since there is no dependence on the variation of the climatic conditions and its behavior was analogous to solar radiation.

Factorial design

The main and the interaction effects with their respective standard errors were calculated with a confidence level of 95%. The Pareto charts for each wavelength are shown in Figure 1. The effects that are considered statistically significant correspond to the bars that extend beyond the line $p = 0.05$.

When analyzing the Pareto charts, it was possible to verify that, for the λ of 411, 625 and 661 nm, all the main and the interaction effects were statistically significant for a 95% confidence level. For the λ of 339 nm all the main and interaction effects were statistically significant at a 95% confidence level minus the interaction effect [H_2O_2] *vs* pH. However, it was necessary to generate the response

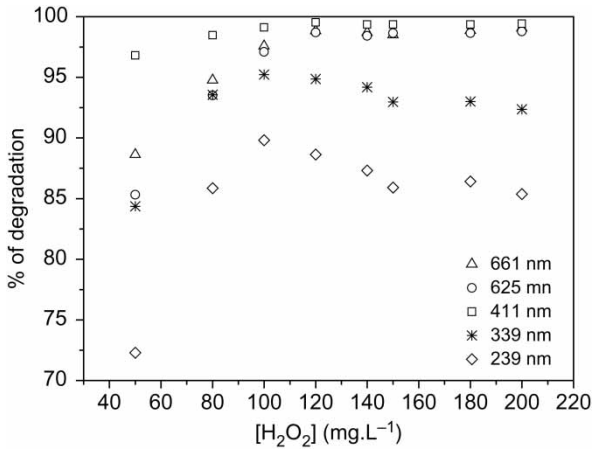

Figure 3 | Optimization of [H_2O_2]. Conditions: [Fe] of 1 mg·L^{-1}, pH 3–4 and time of 1 h.

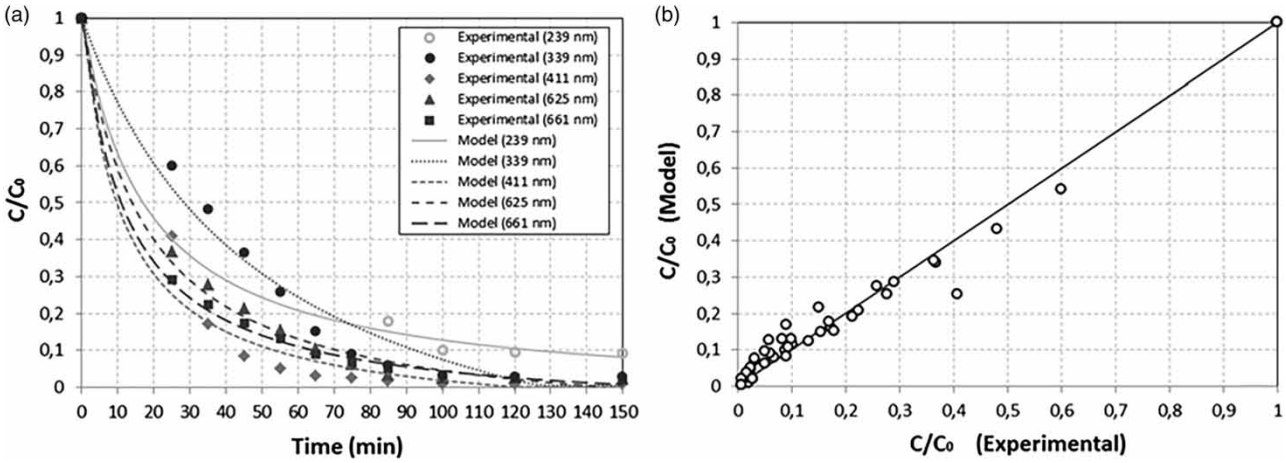

Figure 4 | (a) Adjustment of the experimental data. (b) Experimental values versus values predicted for all λ studied.

surface graph, since the interaction effect between the three factors was significant. For the λ of 239 nm only the main effects [Fe] and pH and interaction [Fe] *vs* pH and [H_2O_2] *vs* pH were statistically significant at a 95% confidence level. For a better understanding of the effects of each of the studied variables, the cube graphs were generated (Figure 2).

The analysis of Figure 2 allowed to verify that for the wavelength equal to 625 and 661 nm the best working conditions were obtained by combining the lower levels of [Fe] and pH, with the highest level of [H_2O_2]. For the λ equal to 441, 339 and 239 nm it was verified that greater percentages of degradation were obtained in the condition of the central point. However, it was observed that for the λ of 411 nm the difference between the percentages of degradation for the center point and the point where there was a greater degradation of the groups seen at 625 and 661 nm is less than 0.2%. Thus, aiming at a greater discoloration of the aqueous solution containing the dyes and considering that there was no significant interaction effect between [H_2O_2]-[Fe] and [H_2O_2]-pH for λ equal to 239 and 339 nm, a univariate study of [H_2O_2] was performed, since the obtained results demonstrate that varying the concentration of this reagent does not influence the degradation of the λ studied.

Optimization of hydrogen peroxide concentration

The results of the hydrogen peroxide concentration optimization study are presented in Figure 3.

It can be seen from Figure 3 that the increase of [H_2O_2] contributes positively to the color degradation up to the concentration of 100 mg·L^{-1}. From this concentration, the values of the percentages of degradation were constant or decreased. Thus, this [H_2O_2] was used in the later trials.

Mousavi *et al.* (2016) studied the influence of [H_2O_2] on Rhodamine B dye degradation and also found that increased [H_2O_2] contributed positively to the color removal. The percentage of dye degradation, at the same time conditions (60 min) and [H_2O_2] (100 mg·L^{-1}), but for an initial dye concentration of 100 mg·L^{-1}, was 55%. Sreeja & Sosamony (2016) argued that the increase in [H_2O_2] leads to a higher rate of mineralization of the dyes studied.

Kinetic study and modeling

With the best working conditions for the degradation of the dyes under study (sunlight, [H_2O_2] equal to 100 mg·L^{-1}, [Fe] equal to 1 mg·L^{-1} and pH between 3 and 4), the kinetic study was performed.

The adjustment of the experimental data to the kinetic model, referring to the temporal advance of the concentration along the oxidation reaction and a comparison between the experimental data and the data predicted by the model through a residue diagram, are shown in Figure 4.

Table 1 | Kinetic and conversion parameters

λ (nm)	X (%)	1/ ρ	1/σ	R^2
239	91	0.057	1.03	0.99
339	97	0.028	1.39	0.95
411	99	0.095	1.09	0.99
625	98	0.065	1.12	0.99
661	98	0.086	1.08	0.99

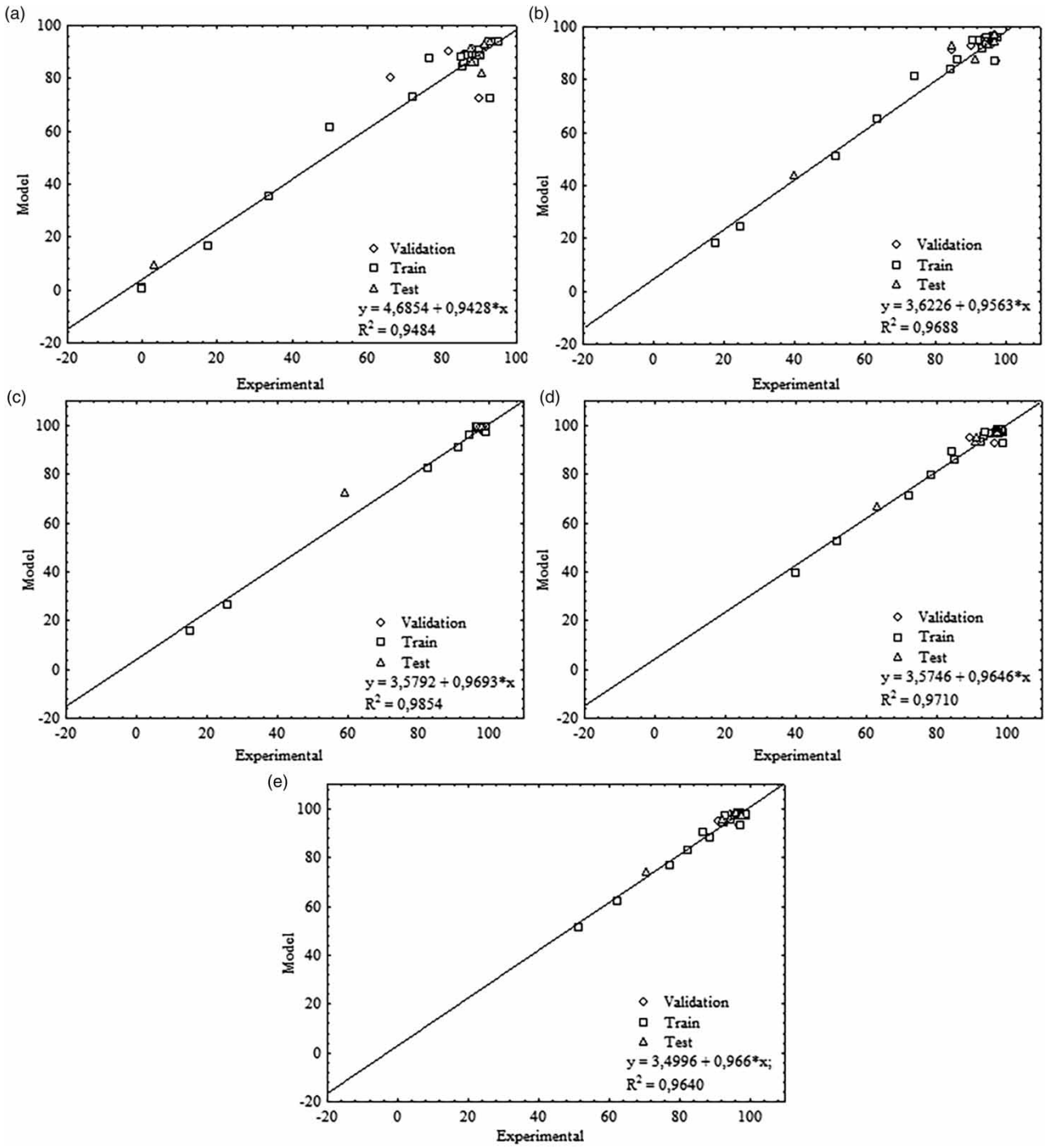

Figure 5 | Linear regressions of the model MLP 4-11-5 for each λ: (a) 239 nm, (b) 339 nm, (c) 411 nm, (d) 625 nm (e) 661 nm.

From Figure 4(a), it can be verified that the photo-Fenton process fit well with the non-linear kinetic model proposed by Chan & Chu (2003). In the first 35 min, a higher rate of degradation occurred, stabilizing after 75 min. It was also found that after 85 min the degradation was greater than 95% for all λ, except for 239 nm, which was 82%, and reaching 91% in 150 min. The residue diagram (Figure 4(b)) reached a good linear regression coefficient with a bisector of 0.985.

The conversion data and kinetic parameters of the oxidation reaction obtained from Equations (1) and (2) can be seen in Table 1.

From Table 1, it was verified that linear regression coefficient (R^2) were above 0.95, indicating a good fit to the proposed model. The reaction rate ($1/\rho$) was higher at the wavelength of 411 nm, characteristic of the RYG dye, obtaining a faster decrease ratio of this compound, as observed in Figure 4. However, the λ of 339 nm characteristic of the TR dye was the one that presented the highest oxidative capacity of the system ($1/\sigma$). These results are in agreement with Paulino *et al.* (2015), which state that the higher the ratio $1/\rho$, the faster the rate of decrease of the compound studied and when t tends to infinity and the value of the constant $1/\sigma$ is equal to the

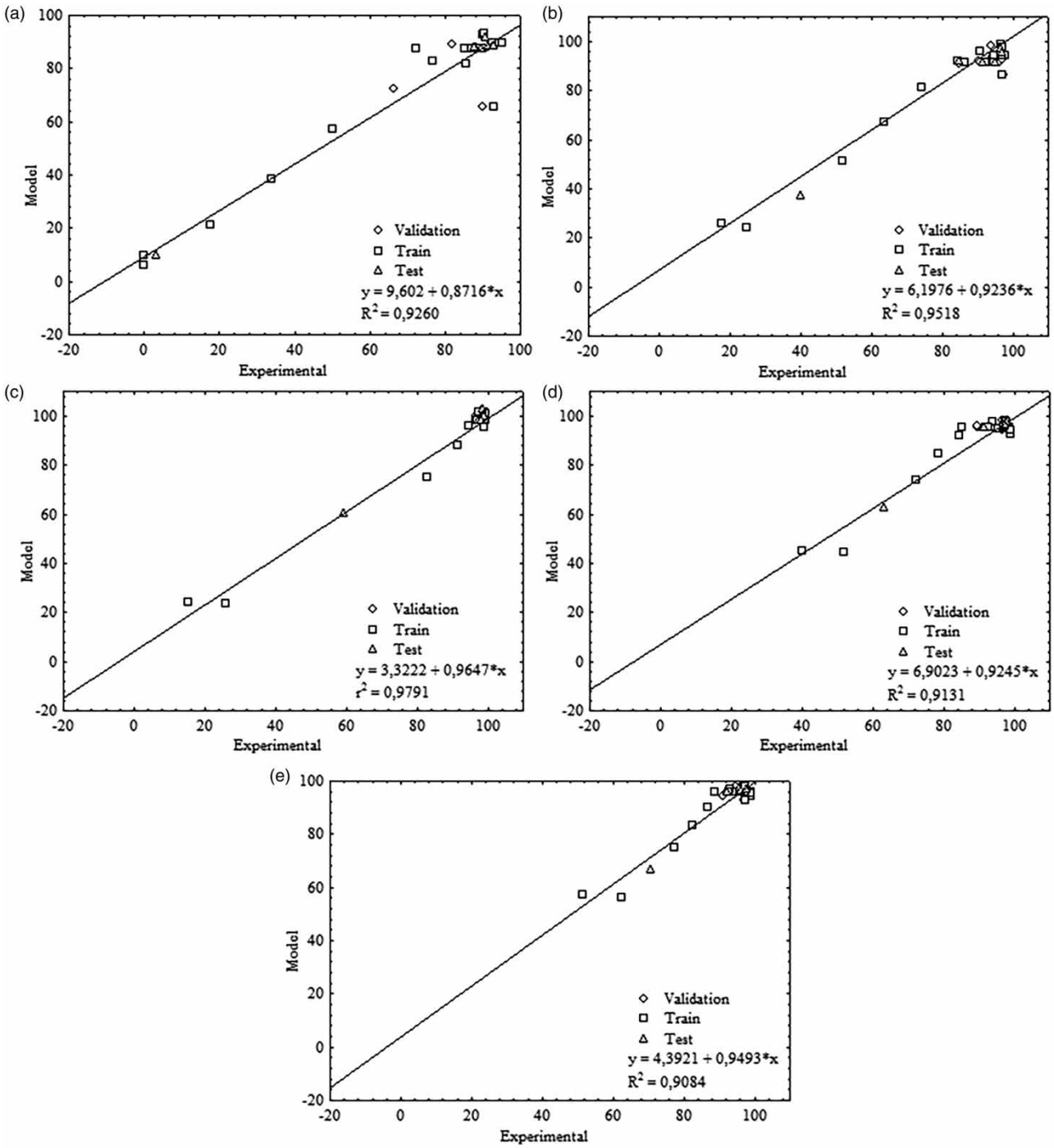

Figure 6 | Linear regressions of the model MLP 4-7-5 for each λ: (a) 239 nm, (b) 339 nm, (c) 411 nm, (d) 625 nm and (e) 661 nm.

Table 2 | Number of germinated seeds, root growth, RGR and GI

Sample	Average number germinated seeds	*M* ± *SD* (cm) of the root growth	*RGR*	*GI (%)*
Water	10.00	7.77 ± 1.43	1.00	100.00
SBT	7.67	6.90 ± 0.95	0.89	68.11
SAT 1%	10.00	7.07 ± 2.25	0.91	90.99
SAT 5%	9.33	7.70 ± 0.35	0.99	92.53
SAT 10%	9.00	7.87 ± 0.81	1.01	91.16
SAT 50%	8.33	6.30 ± 0.75	0.81	67.60
SAT 70%	8.00	3.10 ± 2.59	0.40	31.93
SAT 100%	8.00	3.80 ± 2.91	0.49	39.14

SBT, solution before treatment; SAT, solution after treatment; *M*, mean; *SD*, standard deviation; *RGR*, relative growth index; *GI*, germination index.

maximum oxidation capacity of the process at the end of the reaction.

Artificial neural network modeling

After the simulations performed by Statistica 8.0 software, it was verified that the RBF model did not present a good adjustment of the experimental data. However, the best results were obtained when applying the MLP model: MLP (4-11-5) and MLP (4-7-5). Figures 5 and 6 show the linear regressions of each model.

The analysis of Figures 5 and 6 allowed to verify that the experimental data are adequate to the data simulated by ANN, obtaining a linear regression coefficient above 0.9, as recommended by Cgcre (2003), for both models employed: between 0.9484 and 0.9710 for the MLP (4-11-5) and 0.9084 and 0.9791 for the MLP (4-7-5), indicating that the MLP model (4-11-5) shows a higher accuracy.

Seeds toxicity

The efficiency of the treatment was evaluated by the toxicity of the substances that are formed after submission to AOP under the same treatment conditions described in the kinetic study, using lettuce seeds, *Lactuca sativa*. For this, the number of seeds that germinated was counted and then the root growth study was carried out, as well as, was observed the RGR and the GI. The results are presented in Table 2.

It can be observed from the analysis of Table 2 that the degradation products interfered in the germination and root growth of *Lactuca sativa* seeds, since the values obtained for the negative control (water) were higher. However, it was observed that samples after treatment at concentrations of 1–50% approached the negative control.

Table 3 | Percentage of cell growth and viability after treatment

	Escherichia coli		*Salmonella enteritidis*		
Sample	M ± SD (DO_{600})	Growth (%)	M ± SD (DO_{600})	Growth (%)	Viability
Water	0.124 ± 0.013	100.0	0.271 ± 0.0012	100.0	+
SBT	0.179 ± 0.01	144.3	0.256 ± 0.0024	94.5	+
SAT 1%	0.09 ± 0.009	72.6	0.302 ± 0.0025	111.4	+
SAT 5%	0.099 ± 0.011	79.8	0.293 ± 0.0004	108.1	+
SAT 10%	0.096 ± 0.0007	77.4	0.262 ± 0.0011	96.7	+
SAT 50%	0.005 ± 0.005	4.0	0.006 ± 0.003	2.2	−
SAT 70%	−0.004 ± 0.006	−3.2	0.002 ± 0.008	0.7	−
SAT 100%	0.001 ± 0.008	0.8	0.003 ± 0.00	1.1	−
SAT (10^{-1})	0.111 ± 0.012	89.5	0.281 ± 0.007	103.7	+
SAT 1% (10^{-1})	0.055 ± 0.007	44.3	0.281 ± 0.0095	103.7	+
SAT 5% (10^{-1})	0.079 ± 0.0012	63.7	0.304 ± 0.001	112.2	+
SAT 10% (10^{-1})	0.069 ± 0.0085	55.6	0.28 ± 0.0024	103.3	+
SAT 50% (10^{-1})	0.115 ± 0.005	92.7	0.27 ± 0.003	99.6	+
SAT 70% (10^{-1})	0.142 ± 0.006	114.5	0.279 ± 0.0095	102.9	+
SAT 100% (10^{-1})	0.126 ± 0.00	101.6	0.248 ± 0.004	91.5	+

SBT: solution before treatment; SAT: solution after treatment; *M*: mean; *SD*: standard deviation.

According to Young *et al.* (2012), it is considered that an inhibition of the growth when any of the *RGR* result is below 0.80. Based on this and according to the results presented in Table 2, it was possible to verify that the treated solution showed no toxicity at concentrations below 50%.

Bacteriological toxicity

After the incubation of the samples for 24 h at 36 °C, the count of the CFU·mL^{-1} in relation to the initial inoculum was performed. Then, the percentage of bacterial growth was determined for each of the bacteria under study and the results are presented in Table 3.

The samples after 50, 70 and 100% of degradation showed toxicity to the bacteria *Escherichia coli* and *Salmonella enteritidis*, because there was no growth in the petri dishes after 48 h of incubation, indicating a bactericidal effect. However, when the sample was previously diluted (1:10) in sterile water, this bactericidal effect was not observed and the cells remained viable, indicating a dose-dependent effect.

The presence of toxicity evidenced by the tests using the seeds of *Lactuca sativa* and the bacteria *Escherichia coli* and *Salmonella enteritidis*, even after treatment, may be due to the formation of intermediate compounds that may present higher toxicity than the initial compound.

CONCLUSION

The present study allowed verification that the photo-Fenton system using sunlight radiation presented efficiency above 90% in the treatment of aqueous solution containing the textile dyes Remazol Yellow Gold RNL-150% and Turquoise Reactive Q-G125. From the kinetic study, it was also observed that after 150 min a degradation of more than 97% was reached for the chromophoric groups and 91% for the aromatic compounds. The kinetic study showed that the photo-Fenton process was well suited to the non-linear kinetic model, reaching correlation coefficients above 0.95. From the modeling by ANNs it was verified that the MLP model (4-11-5) presents a better prediction of the experimental data. The toxicity test allowed to verify that in dilutions greater than 50% there is no impairment of both the root growth of the *Lactuca sativa* seeds, as well as of the bacteria *Escherichia coli* and *Salmonella enteritidis*; indicating that after the disposal, the receptor body should not undergo changes in its biota.

ACKNOWLEDGEMENTS

The authors acknowledge Texpal and DyStar companies for providing the dyes, Núcleo de Química Analítica Avançada de Pernambuco (NUQAAPE/FACEPE), FADE/UFPE and CAPES.

REFERENCES

Annadurai, G., Juang, R., Yen, P. & Lee, D. 2003 Use of thermally treated waste biological sludge as dye absorbent. *Advances in Environmental Research* **7** (3), 739–744.

Barros, W. R. P., Franco, P. C., Steter, J. R., Rocha, R. S. & Lanza, M. R. V. 2014 Electro-Fenton degradation of the food dye amaranth using a gás diffusion electrode modified with cobalt (II) phthalocyanine. *Journal of Electroanalytical Chemistry* **722–723**, 46–53.

Barros Neto, B., Scarminio, I. S. & Bruns, R. E. 2007 *Como Fazer Experimentos: Pesquisa E Desenvolvimento na Ciência E na Indústria*. Editora da Unicamp, Campinas, São Paolo, Brazil.

Chan, K. H. & Chu, W. 2003 Modeling the reaction kinetics of Fenton's process on the removal of atrazine. *Chemosphere* **51** (4), 305–311.

Coordenação Geral de Acreditação (CGCRE) 2003 Orientação sobre validação de métodos de ensaios químicos. http://www.inmetro.gov.br/Sidoq/Arquivos/CGCRE/DOQ/DOQ-CGCRE-8_01.pdf (accessed 9 January 2018).

Coordenação Geral de Acreditação (CGCRE) 2016 Orientação sobre validação de métodos analíticos. http://www.inmetro.gov.br/Sidoq/Arquivos/CGCRE/DOQ/DOQ-CGCRE-8_05.pdf (accessed 9 January 2018).

Divya, N., Bansal, A. & Jana, A. 2013 Photocatalytic degradation of azo dye Orange II in aqueous solutions using copper-impregnated titania. *International Journal of Environmental Science and Technology* **10** (6), 1265–1274.

Ertugay, N. & Acar, F. N. 2017 Removal of COD and color from Direct Blue 71 azo dye wastewater by Fenton's oxidation: Kinetic study. *Arabian Journal of Chemistry* **10**, S1158–S1163.

Eskandarloo, H., Badiei, A., Behnajady, M. A. & Ziarani, G. M. 2016 Hybrid homogeneous and heterogeneous photocatalytic processes for removal of triphenylmethane dyes: artificial neural network modeling. *Clean: Soil Air Water* **44** (7), 809–817.

Fahimirad, B., Asghari, A. & Rajabi, M. 2017 Photo-degradation of basic green 1 and basic red 46 dyes in their binary solution by La_2O_3-Al_2O_3 nanocomposite using first-order derivative spectra and experimental design methodology. *Spectrochimica Acta Part A: Molecular and Biomolecular Spectroscopy* **179**, 58–65.

Harris, D. C. 2011 *Análise Química Quantitativa*. LTC, Rio de Janeiro, Brazil.

Le, T. X. H., Nguyen, T. V., Yacouba, Z. A., Zoungrana, L., Avril, F., Petit, E., Mendret, J., Bonniol, V., Bechelany, M., Lacour, S., Lesage, G. & Cretin, M. 2016 Toxicity removal assessments related to degradation pathways of azo dyes:

toward an optimization of electro-Fenton treatment. *Chemosphere* **161**, 308–318.

Lima, D. R. S., Almeida, I. L. A. & Paula, V. 2016 Degradação do corante azul reativo 5G pelo processo oxidativo avançado UV/H_2O_2 (Degradation of the blue 5G reactive dye by the UV/H_2O_2 advanced oxidative process). *E-xacta* **9** (2), 101–109.

Mane, V. S. & Vijay Babu, P. V. 2011 Studies on the adsorption of brilliant green dye from aqueous solution on to low-cost NaOH treated saw dust. *Desalination* **273** (2–3), 321–329.

Mousavi, S. A., Sohrabi, P., Mohammadi, P. & Neyaki, S. M. D. 2016 Investigation of the efficiency UV/H_2O_2 process on the removal of Rhodamine B from aqueous solutions. *International Research Journal of Applied and Basic Sciences* **10** (5), 456–459.

Ozturk, E., Yetis, U., Dilek, F. B. & Demirer, G. N. 2009 A chemical substitution study for a wet processing textile mill in Turkey. *Journal of Cleaner Production* **17** (2), 239–247.

Paulino, T. R. S., Araújo, R. S. & Salgado, B. C. B. 2015 Estudo de oxidação avançada de corantes básicos via reação Fenton (Fe^{2+}/H_2O_2). *Engenharia Sanitaria E Ambiental* **20** (3), 347–352.

Punzi, M., Anbalagan, A., Borner, R. A., Svensson, B.-M., Jonstrup, M. & Mattiasson, B. 2015 Degradation of a textile azo dye using biological treatment followed by photo-Fenton oxidation: evaluation of toxicity and microbial community structure. *Chemical Engineering Journal* **270**, 290–299.

Santana, R. M. R., Nascimento, G. E., Napoleão, D. C. & Duarte, M. M. M. B. 2017 Degradation and kinetic study of Reactive blue BF-5G and Remazol red RB 133% dyes using Fenton and photo-Fenton process. *Revista Eletrônica em Gestão, Educação E Tecnologia Ambiental – REGET* **21** (2), 104–118.

Shu, Z., Bolton, J. R., Belosevic, M. & El Din, M. G. 2013 Photodegradation of emerging micropollutants using the medium-pressure UV/H_2O_2 advanced oxidation process. *Water Research* **47** (8), 2881–2889.

Speck, F., Raja, S., Ramesh, V. & Thivaharan, V. 2016 Modelling and optimization of homogenous photo-Fenton degradation of rhodamine B by response surface methodology and artificial neural network. *International Journal of Environmental Research* **10** (4), 543–554.

Sreeja, P. H. & Sosamony, K. J. 2016 A comparative study of homogeneous and heterogeneous photo-Fenton process for textile wastewater treatment. *Procedia Technology* **24**, 217–223.

Young, B. J., Riera, N. I., Beily, M. E., Bres, P. A., Crespo, D. C. & Ronco, A. E. 2012 Toxicity of the effluent from an anaerobic bioreactor treating cereal residues on *Lactuca sativa*. *Ecotoxicology and Environmental Safety* **76** (2), 182–186.

Zaidan, L. E. M. C., Pinheiro, R. B., Santana, R. M. R., Charamba, L. V. C., Napoleão, D. C. & Silva, V. L. 2017 Evaluation of efficiency of advanced oxidative process in degradation of 2-4 dichlorophenol employing UV-C radiation reator. *Revista Eletrônica em Gestão, Educação E Tecnologia Ambiental – REGET* **21** (2), 147–157.

First received 10 January 2018; accepted in revised form 23 May 2018. Available online 4 June 2018